

On Optimizing the Power Allocation and the Decoding Order in Uplink Cooperative NOMA

Mohamed Elhattab, Mohamed Amine Arfaoui, Chadi Assi, Ali Ghrayeb, and Marwa Qaraqe

Abstract—In this paper, we investigate for the first time the dynamic power allocation and decoding order at the base station (BS) of two-user uplink (UL) cooperative non-orthogonal multiple access (C-NOMA)-based cellular networks. In doing so, we formulate a joint optimization problem aiming at maximizing the minimum user achievable rate, which is a non-convex optimization problem and hard to be directly solved. To tackle this issue, an iterative algorithm based on successive convex approximation (SCA) is proposed. The numerical results reveal that the proposed scheme provides the superior performance in comparison with the traditional UL NOMA. In addition, we demonstrated that in UL C-NOMA, decoding the far NOMA user first at the BS provides the best performance.

Index Terms—C-NOMA, Fairness, Power allocation, Uplink.

I. INTRODUCTION

Non-orthogonal multiple access (NOMA) has been envisioned as a candidate multiple access technique for next-generation wireless networks [1]. The main idea of NOMA is to allow multiple user equipment (UEs) to access the same resource block (a time slot, a spreading code, or a frequency band), but with different power levels [1]. Specifically, NOMA utilizes superposition coding (SC) at the transmitter with proper power allocation as well as successive interference cancellation (SIC) at the receiver to cancel the inter-NOMA user interference [1]. It has been shown that NOMA outperforms the traditional orthogonal multiple access (OMA) techniques from the aspect of network connectivity and network spectral efficiency in both downlink (DL) and uplink (UL) transmissions [2].

In order to further improve the performance of NOMA cellular networks with low-cost infrastructure, the integration between NOMA and user-cooperative relaying referred to as cooperative NOMA (C-NOMA) has been developed [3]. In C-NOMA, the near NOMA UEs, with typically good channel conditions, act as relays to assist the transmission of far NOMA UEs, who generally have bad channel conditions [3]. As a result, by adding a cooperative link between a near NOMA UE and a far NOMA UE, a new degree of diversity alongside the base station (BS)-UEs link is introduced, thus allowing C-NOMA based wireless networks to achieve better fairness and higher spectral efficiency as compared to NOMA. [3].

Many work have investigated the performance of C-NOMA-based cellular networks and evaluated its performance in comparison with NOMA in terms of minimum user achievable rate [3], network sum-rate [4], outage probability [5], secrecy performance [6] and network power consumption [7]. Specifically, the authors in [3] studied the power allocation to maximize the minimum UE achievable rate for a two-UE downlink C-NOMA network. The authors in [4] discussed joint user pairing and power allocation to maximize the network sum-rate. The

integration between coordinated multipoint transmission and C-NOMA was studied in [5] to improve the outage probability of the far NOMA UEs. Finally, the integration between C-NOMA and reconfigurable intelligent surface was analyzed to minimize the network power consumption in [7].

It is worth mentioning that the aforementioned work and the citations therein solely investigate the potential gains of C-NOMA in the DL scenario, whereas research on its UL counterpart is still in its infancy stage. Recently, there has been a few work that focused on investigating the performance of UL C-NOMA networks [8]–[10]. The authors in [8] and [9] studied the performance analysis in terms of the ergodic capacity and the outage probability in a two-UE UL C-NOMA network, respectively, where [8] considered a dedicated full-duplex (FD) decode and forward (DF) relay; meanwhile [9] considered a dedicated half-duplex (HD) DF relay to assist the transmission of the two UL UEs. In addition, the authors in [8] and [9] assumed that there were no communication links between the BS and the UEs. In contrast, the authors in [10] analyzed the performance of a two-UE UL C-NOMA in terms of the outage probability and the network sum-rate and considered a *user cooperating relay* in which the near NOMA UE acted as a FD DF relay to assist the transmission from the far NOMA UE to the BS. However, all the aforementioned work studied only the performance analysis of an UL two-UE C-NOMA network while assuming a fixed non-optimal power control scheme.

To the best of our knowledge, the dynamic power allocation in an UL two-UE C-NOMA network is yet to be investigated, thus motivating the study of this paper. Specifically, our main objective in this paper is to address the following questions.

- **Q1:** What is the impact of employing a dynamic power allocation on the performance of UL C-NOMA over traditional UL NOMA?
- **Q2:** What is the appropriate decoding order in UL C-NOMA cellular networks?
- **Q3:** What are the main system parameters that emphasize the indispensability of invoking UL C-NOMA in cellular networks?

In order to answer the above questions, we consider a two-UE UL C-NOMA system consisting of one BS, one near NOMA UE, denoted as UE_n , and one far NOMA UE, denoted as UE_f , in which UE_n acts a FD DF relay to assist the transmission from the UE_f to the BS. Specifically, we examine the impact of performing a dynamic power allocation and changing decoding order at the BS. In doing so, we formulate a power allocation problem to optimize the power allocation coefficients at UE_n and the transmit power at UE_f with the goal of maximizing the minimum UE's rate. Furthermore, we investigate two different SIC decoding orders at the BS, namely, far NOMA UE decoded first and near NOMA UE decodes first. The formulated optimization problem is a non-convex problem, which is difficult

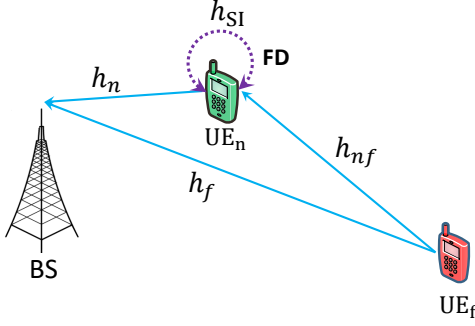


Fig. 1. UL C-NOMA System Model

to be solved directly. To tackle this challenge, we propose a successive convex approximation (SCA)-based iterative algorithm to effectively solve the formulated optimization problem. We demonstrate the efficacy of the proposed algorithm by comparing its performance with the traditional UL NOMA. Our findings reveal that decoding the data of the far NOMA UE first always provides the best performance. Moreover, it is shown that the transmit power at far NOMA UE, the channel gain between the far and near NOMA UEs, and the self-interference channel have significant impact on the performance of UL C-NOMA.

II. SYSTEM, TRANSMISSION AND SIGNAL MODELS

A. Network Model

We consider an UL transmission in a two-UE C-NOMA cellular network, which consists of one BS, one UE_n and one UE_f as shown in Fig. 1. Similar to [3], [11], we assume that the UEs and the BS each has one transmit and one receive antenna. Based on the NOMA principle, UE_n and UE_f can be served in the same resource (frequency/time) and form a NOMA pair. In order to enhance the performance of the traditional UL NOMA scheme, in this paper, we allow the UE_n to assist the transmission of UE_f by relaying the UE_f 's message through a FD DF relaying mode.

To this end, there are three wireless communication links, namely, $UE_n \rightarrow BS$, $UE_f \rightarrow BS$, and $UE_f \rightarrow UE_n$, whose channel coefficients are denoted, respectively, by h_n , h_f , and h_{nf} . In addition, there is a self-interference (SI) link arising from $UE_n \rightarrow UE_n$, whose channel coefficient is denoted by h_{SI} . This SI is caused by the simultaneous transmission and reception at UE_n . All wireless channels as well as the SI channel are independent and follow a Rayleigh distribution. Consequently, the channel gains for those wireless links follow Exponential distributions with parameters λ_n , λ_f , and λ_{nf} , respectively, and λ_{SI} for the SI link. Finally, we denote the power budget of the UE_n and UE_f by P_n^{\max} and P_f^{\max} , respectively.

B. Transmission Model and Decoding Orders

The transmission scheme in the considered model consists of two phases, described as follows.

- *First Phase:* UE_f broadcasts its own message, which is received by both the BS and the UE_n .
- *Second Phase:* UE_n first decodes the message of UE_f , then it superimposes its own message with the decoded message of UE_f using SC. Finally, UE_n transmits the superimposed signal to the BS.

Since UE_n adopts FD relaying mode, the two phases are executed within the same time-slot at the cost of the induced SI at the UE_n [4]. Next, we discuss the possible decoding orders at the BS to detect the signals of UE_n and UE_f . In this model, there are two possible decoding orders explained as follows.

- 1) *Far user decoded first (FUDF):* This decoding order is similar to the one applied in downlink NOMA/C-NOMA networks [2], [4]. Specifically, the BS decodes the UE_f 's message first considering the UE_n 's signal as an interference signal. Then, the BS removes the signal of UE_f from its received signal to decode the message of UE_n without interference.
- 2) *Near user decoded first (NUDF):* This is the most widely used decoding order for UL NOMA transmission [2]. In this case, the BS first decodes the message of UE_n considering the UE_f 's message as an interference signal. Subsequently, the BS decodes the message of UE_f free of interference.

C. Signal Model

We start by describing the signal model at UE_n due to the transmission of UE_f . Then, we discuss the signal model due to the transmission of both UE_n and UE_f at the BS. First, the received signal at UE_n in the t th time slot due to the transmission of UE_f can be written as follows,

$$y_{n,1} = \left(\sqrt{\beta_f^{[m]} P_f^{\max}} h_{nf} x_f[t] + \sqrt{(\alpha_n^{[m]} + \alpha_f^{[m]}) P_n^{\max}} h_{SI} x_s[t - \tau] \right) + w_n[t], \quad (1)$$

where $x_s[t - \tau] = \alpha_n^{[m]} x_n + \alpha_f^{[m]} x_f$ is the superimposed signal at the UE_n , $\alpha_n^{[m]}, \alpha_f^{[m]} \in [0, 1]$ are the power allocation coefficients for the m th decoding order that the UE_n assigns to transmit its own message and the message of UE_f , respectively, and $\beta_f^{[m]} \in [0, 1]$ is the fraction of power that UE_f utilizes from its power budget to transmit its own data. Moreover, $m \in \{1, 2\}$ represents the decoding order where $m = 1$ indicates the decoding order is FUDF and $m = 2$ indicates the decoding order is NUDF, w_n is the additive white Gaussian noise with zero mean and variance of σ^2 , and τ is the processing delay at UE_n , which is assumed to be smaller than the time slot t [4], [12]. Based on this, the received signal-to-interference-plus-noise-ratio (SINR) at UE_n to detect x_f can be expressed as

$$\delta_{n \rightarrow f}^{[m]} = \frac{\beta_f^{[m]} P_f^{\max} \gamma_{nf}}{(\alpha_n^{[m]} + \alpha_f^{[m]}) P_n^{\max} \gamma_{SI} + 1}, \quad (2)$$

where $\gamma_{nf} = |h_{nf}|^2 / \sigma^2$ and $\gamma_{SI} = |h_{SI}|^2 / \sigma^2$. Consequently, the achievable rate at UE_n to decode the signal of UE_f can be expressed as $\mathcal{R}_{n \rightarrow f}^{[m]} = \log(1 + \delta_{n \rightarrow f}^{[m]})$. On the other hand, in the second phase, UE_n superimposes the decoded signal of UE_f , i.e. x_f , and its own message x_n , and then transmits this superimposed signal to the BS considering FD DF relaying

mode. Consequently, at the end of the second phase, the received signal at the BS can be written as follows,

$$y_{b,2} = \underbrace{\sqrt{\alpha_n^{[m]} P_n^{\max}} x_n[t - \tau] + \sqrt{\alpha_f^{[m]} P_f^{\max}} x_f[t - \tau]}_{\text{Received signal from UE}_n \text{ (second phase)}} + \underbrace{\sqrt{\beta_f^{[m]} P_f^{\max}} h_f x_f[t]}_{\text{Received signal from UE}_f \text{ (first phase)}} + w_b[t], \quad (3)$$

It is worth mentioning that the SINR and the achievable rate expressions for both UE_n and UE_f at the BS depend on the decoding order that the BS applies. Therefore, we discuss the SINR and rate expressions for both the FUDF and the NUDF schemes in the following section.

III. SINR AND RATE EXPRESSIONS

A. SINR and Rate Expressions for the FUDF Scheme

In this scheme, the BS starts by decoding first the message of UE_f considering the transmission of UE_n to its own message as an interference signal. It is clear that the BS receives the message of UE_f from both UE_f and UE_n. As a result, at the end of the second phase, the BS employs the maximum ratio combining (MRC) technique to combine these receptions in order to decode the message of UE_f [4]. Then, the interference signal caused by the signal of UE_f will be subtracted from the received signals using the SIC process to decode the message of UE_n. Consequently, the SINR for decoding UE_f's message as well as the signal-to-noise-ratio (SNR) for decoding the UE_n's message are given, respectively, by

$$\delta_f^{[1]} = \frac{\alpha_f^{[1]} P_n^{\max} \gamma_n}{\alpha_n^{[1]} P_n^{\max} \gamma_n + 1} + \beta_f^{[1]} P_f^{\max} \gamma_f, \quad (4)$$

$$\delta_n^{[1]} = \alpha_n^{[1]} P_n^{\max} \gamma_n, \quad (5)$$

where $\gamma_f = |h_f|^2/\sigma^2$ and $\gamma_n = |h_n|^2/\sigma^2$. Finally, the achievable data rate of UE_n as well as UE_f at the BS can be, respectively, expressed as

$$\mathcal{R}_n^{[1]} = \log(1 + \delta_n^{[1]}), \text{ and } \mathcal{R}_f^{[1]} = \min(\mathcal{R}_{n \rightarrow f}^{[1]}, \mathcal{R}_{\text{sum}}^{[1]}), \quad (6)$$

where $\mathcal{R}_{\text{sum}}^{[1]} = \log_2(1 + \delta_f^{[1]})$. It is important to mention that since UE_n employs DF relaying, the achievable rate for UE_f is the minimum between $\mathcal{R}_{n \rightarrow f}^{[1]}$ and $\mathcal{R}_{\text{sum}}^{[1]}$ [4].

B. SINR and Rate Expressions for the NUDF Scheme

Different from the FUDF scheme, the UE_n is decoded first at the BS in the NUDF scheme, and hence, the received signal of the UE_f acts as an interference signal and its SINR at the BS to decode its own message can be expressed as

$$\delta_n^{[2]} = \frac{\alpha_n^{[2]} P_n^{\max} \gamma_n}{\alpha_f^{[2]} P_n^{\max} \gamma_n + \beta_f^{[2]} P_f^{\max} \gamma_f + 1}. \quad (7)$$

Based on this, the achievable data rate of UE_n at the BS can be expressed as $\mathcal{R}_n^{[2]} = \log(1 + \delta_n^{[2]})$. After the BS decodes the message of UE_n, it removes it from the received signal to decode the message of UE_f without interference with the following SINR

$$\delta_f^{[2]} = \alpha_f^{[2]} P_n^{\max} \gamma_n + \beta_f^{[2]} P_f^{\max} \gamma_f. \quad (8)$$

Hence, the achievable rate of UE_f at the BS is expressed as

$$\mathcal{R}_f^{[2]} = \min(\mathcal{R}_{n \rightarrow f}^{[2]}, \mathcal{R}_{\text{sum}}^{[2]}), \quad (9)$$

where $\mathcal{R}_{\text{sum}}^{[2]} = \log(1 + \delta_f^{[2]})$.

IV. PROPOSED POWER CONTROL SCHEME: PROBLEM FORMULATION AND SOLUTION APPROACH

A. Problem Formulation

In this paper, we emphasize the user fairness issue. Specifically, we investigate the joint optimization of the power allocation coefficients at UE_n, i.e. $\alpha_n^{[m]}$ and $\alpha_f^{[m]}$, and the power allocation fraction at UE_f, i.e., $\beta_f^{[m]}$, with the objective of maximizing the minimum user rate. The max-min rate optimization problem for a two-UE UL C-NOMA system is formulated as¹

$$\text{OPT : } \max_{\alpha_n^{[m]}, \alpha_f^{[m]}, \beta_f^{[m]}} \min(\mathcal{R}_f^{[m]}, \mathcal{R}_n^{[m]}) \quad (10a)$$

$$\text{s.t. } 0 \leq \alpha_n^{[m]} + \alpha_f^{[m]} \leq 1, \quad (10b)$$

$$0 \leq \beta_f^{[m]} \leq 1, \quad (10c)$$

where constraints (10b) and (10c) ensure that the transmit powers at UE_n and at UE_f do not exceed their power budgets, i.e., P_n^{\max} and P_f^{\max} , respectively. It can be seen that problem OPT is neither concave nor quasi-concave, which is difficult to be directly solved. In the next section, we present the solution approach when the adopted decoding order at the BS is FUDF, i.e. $m = 1$.²

B. Solution Approach

By introducing an auxiliary variable ζ , the power control optimization problem can be rewritten as follows

$$\mathcal{P} : \max_{\alpha_n^{[1]}, \alpha_f^{[1]}, \beta_f^{[1]}} \zeta \quad (11a)$$

$$\text{s.t. } (10b), (10c), \quad (11b)$$

$$\log(1 + \alpha_n^{[1]} P_n^{\max} \gamma_n) \geq \zeta, \quad (11c)$$

$$\log\left(1 + \frac{\alpha_f^{[1]} P_n^{\max} \gamma_n}{\alpha_n^{[1]} P_n^{\max} \gamma_n + 1} + \beta_f^{[1]} P_f^{\max} \gamma_f\right) \geq \zeta, \quad (11d)$$

$$\log\left(1 + \frac{\beta_f^{[1]} P_f^{\max} \gamma_n}{(\alpha_n^{[1]} + \alpha_f^{[1]}) P_n^{\max} \gamma_{\text{SI}} + 1}\right) \geq \zeta. \quad (11e)$$

It can be observed that problem \mathcal{P} is a non-convex optimization problem due to the non-convex constraints (11d) and (11e). In order to tackle this challenge, we first reformulate constraints (11d) and (11e), respectively, as follows.

$$\alpha_f^{[1]} P_n^{\max} \gamma_n + \alpha_n^{[1]} \beta_f^{[1]} P_n^{\max} P_f^{\max} \gamma_n \gamma_f + \beta_f^{[1]} P_f^{\max} \gamma_f \geq \vartheta \alpha_n^{[1]} P_n^{\max} \gamma_n + \vartheta, \quad (12)$$

$$\beta_f^{[1]} P_f^{\max} \gamma_n \gamma_f \geq (\alpha_n^{[1]} \vartheta + \alpha_f^{[1]} \vartheta) P_n^{\max} \gamma_{\text{SI}} + \vartheta, \quad (13)$$

where ϑ is an auxiliary variable that should achieve the condition $\vartheta \geq \exp(\zeta) - 1$. Nevertheless, both (12) and (13) are intractable due to the multiplication of the two variables that exists in the left and right sides of those constraints. According to [13], in order to tackle the multiplication of the variables in

¹In a multi-user scenario, an optimal UEs pairing policy should be first discussed to cluster one UE_n with one UE_f. One can obtain the optimal pairing scheme using the Hungarian method [4]. Then, the proposed power control scheme is applied for each NOMA pair to maximize the minimum user achievable rate in that pair. Note that, different NOMA pairs are served through orthogonal resources to avoid the inter-NOMA pair interference [4].

²It is worth mentioning that the optimization problem OPT when $m = 2$ can be similarly solved by following the same steps in section IV-B.

the right hand side of those constraints, and for any non-negative variables x, y , and z , the approximation of the following expression $xy \leq z$ can be formulated as $2xy \leq (ax)^2 + (y/a)^2 \leq 2z$, where the first inequality holds if and only if $a = \sqrt{y/x}$. Based on this, equations (12) and (13) can be rewritten as follows

$$\alpha_f^{[1]} P_n^{\max} \gamma_n + \alpha_n^{[1]} \beta_f^{[1]} P_n^{\max} P_f^{\max} \gamma_n \gamma_f + \beta_f^{[1]} P_f^{\max} \gamma_f \geq v P_n^{\max} \gamma_n + \vartheta, \quad (14)$$

$$\beta_f^{[1]} P_f^{\max} \gamma_{nf} \geq (v + u) P_n^{\max} \gamma_{SI} + \vartheta, \quad (15)$$

where the auxiliary variables u and v should satisfy the following constraints

$$\left(\frac{\alpha_n^{[1]}}{b^{[r]}} \right)^2 + \left(\vartheta b^{[r]} \right)^2 \leq 2v, \text{ and } \left(\frac{\alpha_f^{[1]}}{a^{[r]}} \right)^2 + \left(\vartheta a^{[r]} \right)^2 \leq 2u, \quad (16)$$

such that $b^{[r]}$ and $a^{[r]}$ denote the values of b and a in the r th iteration, which can be updated by

$$b^{[r]} = \sqrt{\frac{\alpha_n^{[1,r]}}{\vartheta^{[r]}}} \text{ and } a^{[r]} = \sqrt{\frac{\alpha_f^{[1,r]}}{\vartheta^{[r]}}}, \quad (17)$$

After the previous approximation, one can see that (15) is a convex constraint. However, (14) is still non-convex due to the variables multiplication in the left hand side. In order to handle this challenge, we introduce an auxiliary variable Λ and equivalently define the following constraints

$$v P_n^{\max} \gamma_n + \vartheta - \alpha_f^{[1]} P_n^{\max} \gamma_n - \Lambda^2 P_n^{\max} P_f^{\max} \gamma_n \gamma_f - \beta_f^{[1]} P_f^{\max} \gamma_f \leq 0 \quad (18)$$

$$\alpha_n^{[1]} \beta_f^{[1]} \geq \Lambda^2. \quad (19)$$

Here, (19) is a quadratic conic convex constraint, meanwhile (18) is non-convex due to the concave function $f(\Lambda) = -\Lambda^2$ which renders the right side of (18) as a difference-of-convex (DC) form. Thus, with $\Lambda^{[r]}$ as the input point, we can apply the SCA technique to replace $f(\Lambda)$ by its first order Taylor approximate as:

$$\tilde{f}(\Lambda; \Lambda^{[r]}) = -(\Lambda^{[r]})^2 - 2\Lambda^{[r]}(\Lambda - \Lambda^{[r]}). \quad (20)$$

At this point, problem \mathcal{P} can then be replaced by:

$$\mathcal{P}_1 : \max_{\alpha_n^{[1]}, \alpha_f^{[1]}, \beta_f^{[1]}, v, \vartheta, \zeta, \Lambda, u} \zeta \quad (21a)$$

$$\text{s.t.} \quad (10b), (10c), (15), (16), (19), \quad (21b)$$

$$\vartheta \geq \exp(\zeta) - 1, \quad (21c)$$

$$\alpha_n^{[1]} P_n^{\max} \gamma_n \geq \vartheta, \quad (21d)$$

$$v P_n^{\max} \gamma_n + \vartheta + P_n^{\max} P_f^{\max} \gamma_n \gamma_f \tilde{f}(\Lambda; \Lambda^{[m]}) - \alpha_f P_n^{\max} \gamma_n - \beta_f P_f^{\max} \gamma_f \leq 0. \quad (21e)$$

One can remark that the obtained problem \mathcal{P}_1 is a generalized convex problem due to the existence of the generalized exponential cone constraints (21c). Although \mathcal{P}_1 can be efficiently solved using a convex solver [14], it generally entails more computational time in comparison with other standard convex programs such as second order cone programming (SOCP) [14]. As a result, a conic programming solver may be used to provide a much more efficient practical implementation while achieving

Algorithm 1: Proposed Algorithm

- 1 **Input:** channel gains $h_n, h_f, h_{n,f}, h_{SI}, \sigma^2, P_f^{\max}, P_n^{\max}$, decoding order m , maximum number of iteration N , and maximum tolerance $\epsilon = 10^{-4}$;
 - 2 **Initialize:** Iteration index $r = 1$, $b^{[0]}, a^{[0]}$, and $\Lambda^{[0]}$;
 - 3 **while** $r \leq N$ and $\zeta^{[r+1]} - \zeta^{[r]} > \epsilon$ **do**
 - 4 Increment $r := r + 1$;
 - 5 Obtain the values of $\alpha_n^{[m,r]}, \alpha_f^{[m,r]}, \beta_f^{[m,r]}, \vartheta^{[r]}, \zeta^{[r]}, u^{[r]}$, and $v^{[r]}$ by solving problem \mathcal{P}_2 ;
 - 6 Update $\Lambda^{[r]}$;
 - 7 Update $a^{[r]}$, and $b^{[r]}$ based on (17);
 - 8 **Output:** $\alpha_n^{[1]}, \alpha_f^{[1]}, \beta_f^{[1]}$, and ζ ;
-

an accuracy of 99.99% [14]. Consequently, this motivates us to invoke the conic approximation with controlled accuracy in which constraint (21c) can be rewritten by a set of second order cone inequalities as [14]:

$$\kappa_{q+4} \leq 1 + \vartheta \quad (22)$$

$$\begin{aligned} 1 + \kappa_1 &\geq \left\| \begin{bmatrix} 1 - \kappa_1 & 2 + \zeta/2^{q-1} \end{bmatrix} \right\|_2 \\ 1 + \kappa_2 &\geq \left\| \begin{bmatrix} 1 - \kappa_2 & 5/3 + \zeta/2^q \end{bmatrix} \right\|_2 \\ 1 + \kappa_3 &\geq \left\| \begin{bmatrix} 1 - \kappa_3 & 2\kappa_1 \end{bmatrix} \right\|_2 \\ \kappa_4 &\geq \kappa_2 + \kappa_3/24 + 19/72 \\ 1 + \kappa_l &\geq \left\| \begin{bmatrix} 1 - \kappa_l & 2\kappa_{l-1} \end{bmatrix} \right\|_2 \quad \forall l \in \{5, \dots, q+3\} \\ 1 + \kappa_{q+4} &\geq \left\| \begin{bmatrix} 1 - \kappa_{q+4} & 2\kappa_{q+3} \end{bmatrix} \right\|_2 \end{aligned} \quad (23)$$

where $\kappa_q, \forall q \in \{0, 1, \dots, q+4\}$ is a new slack variable and q is the parameter of the conic approximation technique to control the accuracy of the approximation, which can be chosen, according to [14], as $q = 4$ to achieve around 99.99% accuracy. Towards this end, problem \mathcal{P}_1 can be rewritten as

$$\mathcal{P}_2 : \max_{\alpha_n^{[1]}, \alpha_f^{[1]}, \beta_f^{[1]}, v, \vartheta, \zeta, \Lambda, u, \kappa_q} \zeta \quad (24a)$$

s.t. (10b), (10c), (15), (16), (19), (21d), (21e), (22), and (23).

Based on the above analysis, we can see that all the constraints in problem \mathcal{P}_2 are either linear or quadratic conic convex constraints. Hence, it can be efficiently solved using a standard optimization solver such as MOSEK [14]. Finally, the proposed iterative algorithm is presented in **Algorithm 1**, where in each iteration, we solve \mathcal{P}_2 for given values of $\Lambda^{[r]}, a^{[r]}$, and $b^{[r]}$ to obtain the optimal values of $\alpha_n^{[m]}, \alpha_f^{[m]}, \beta_f^{[m]}, \vartheta, \zeta, u$, and v . Then, we update the iteration index r and the parameters $\Lambda^{[r]}, a^{[r]}$, and $b^{[r]}$ to solve \mathcal{P}_2 in the next iteration until the condition either $r > N$ or $(\zeta^{[r+1]} - \zeta^{[r]}) \leq \epsilon$ is satisfied.

V. SIMULATION RESULTS AND DISCUSSION

In this section, our objective is to analyze the performance of the two proposed decoding schemes, FUDF and NUDF, under various system parameters by varying the power budget at UE_n , the power budget at UE_f , the SI channel gain, and the channel gain between UE_n and UE_f . The simulation results are obtained through generating 10^3 independent Monte-Carlo trials. Unless otherwise mentioned, we adopt the same simulation setting in [3], in which $\lambda_n = \lambda_{nf} = 12$ dB, $\lambda_f = 3$ dB, and $\lambda_{SI} = 5$ dB. In order to highlight the effectiveness of the proposed schemes,

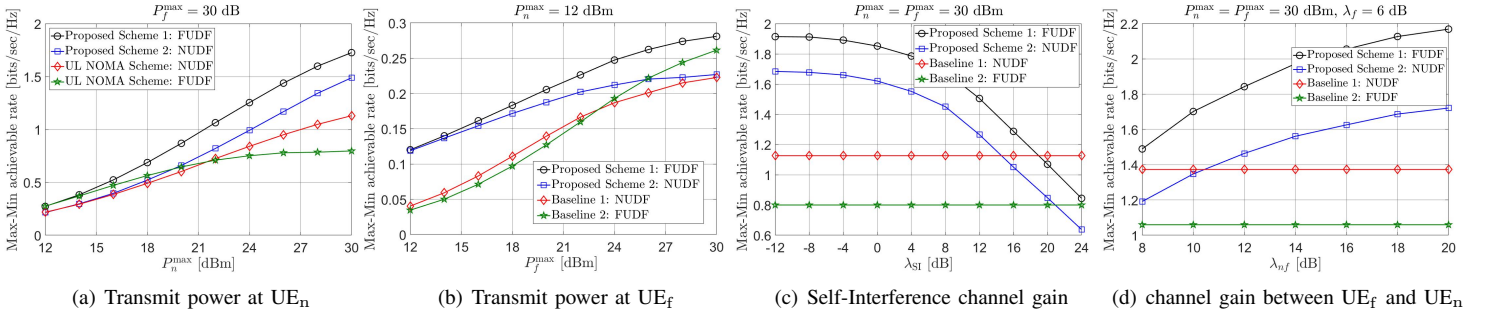


Fig. 2. Performance evaluation of the proposed UL C-NOMA transmission.

we compare them with the two following baselines that are based on the traditional UL NOMA scheme [2], [15].

- 1) *UL NOMA considering NUDF approach*: This scheme is denoted as baseline 1 in which UE_n is decoded first at the BS.
- 2) *UL NOMA considering FUDF approach*: This scheme is denoted as baseline 2 in which UE_f is decoded first at the BS.

First, one can see from Fig. 2 that the proposed FUDF scheme achieves the best performance compared to the other proposed NUDF scheme as well as the two considered baselines schemes. This observation is different from the traditional UL NOMA scheme [2], where, in the majority of the cases, decoding the near user first (baseline 1) is better than decoding the far user first (baseline 2). This advises that the BS should always decode the far user first in UL C-NOMA networks.

Fig. 2(a) depicts the effect of increasing the power budget at UE_n on the performance of the four schemes. It can be seen that at a low power budget at UE_n and a high power budget at UE_f , the FUDF scheme almost achieves the same performance as baseline 2. This is because most of the power of the UE_n is assigned to its own message rather than UE_f 's message in order to improve its performance, since the high power budget at UE_f substitutes its weak channel with the BS. However, when P_n^{\max} increases, the proposed FUDF achieves a higher performance gain compared to the two baselines schemes. This is because increasing P_n^{\max} motivates UE_n to assist UE_f and, hence, improves the performance of both UE_n and UE_f .

Fig. 2(b) presents the effect of P_f^{\max} on the system performance. Note that, when P_f^{\max} is low, the cooperation between UE_n and UE_f is indispensable. The main reason behind this is that the received signal at the BS due to the transmission of UE_f is weak and UE_n should assist the transmission to improve UE_f 's achievable rate. On the other hand, when P_f^{\max} increases, and since P_n^{\max} is low, UE_n starts to allocate most of its power to its own message and, hence, the performance gains due to the cooperation diminishes. Fig. 2(c) shows the effect of SI channel gain on the C-NOMA schemes. Increasing the SI channel gain forces UE_n to reduce its transmit power so that it can avoid harming itself. As a result, when the SI values is relatively large, UE_n transmits with very low power and the performance of the UL C-NOMA becomes worse than that of UL NOMA. Finally, Fig. 2(d) presents the effect of λ_{nf} on the system performance. It can be seen that the performance gain between C-NOMA and NOMA when the cooperative link has a bad channel condition is low. This is reasonable because C-NOMA mainly depends on

the cooperative link. Meanwhile, when λ_{nf} is relatively good, the performance of the DF relaying enhances and, hence, the minimum user rate improves.

VI. CONCLUSION

In this paper, we investigated the performance of the UL C-NOMA and compared its performance with the traditional UL NOMA. In contrast to UL NOMA technique, we have shown that the BS should always decode first the far user's message. In addition, we have also observed that UL C-NOMA achieves a superior performance compared to UL NOMA, especially with low power budget at far NOMA user, moderate values for the SI channel, and with good channel conditions between the far NOMA user and the near NOMA user.

REFERENCES

- [1] L. Dai *et al.*, "A Survey of Non-Orthogonal Multiple Access for 5G," *IEEE Commun. Surveys Tuts.*, vol. 20, no. 3, pp. 2294–2323, 2018.
- [2] M. S. Ali *et al.*, "Dynamic User Clustering and Power Allocation for Uplink and Downlink Non-Orthogonal Multiple Access (NOMA) Systems," *IEEE Access*, vol. 4, pp. 6325–6343, Aug. 2016.
- [3] G. Liu *et al.*, "Hybrid Half-Duplex/Full-Duplex Cooperative Non-Orthogonal Multiple Access With Transmit Power Adaptation," *IEEE Trans. Wireless Commun.*, vol. 17, no. 1, pp. 506–519, Jan. 2018.
- [4] P. H  u *et al.*, "A Low-Complexity Framework for Joint User Pairing and Power Control for Cooperative NOMA in 5G and Beyond Cellular Networks," *IEEE Trans. Commun.*, vol. 68, pp. 6737–6749, Nov. 2020.
- [5] M. Elhattab, M. A. Arfaoui, and C. Assi, "A Joint CoMP C-NOMA for Enhanced Cellular System Performance," *IEEE Commun. Lett.*, vol. 24, no. 9, pp. 1919–1923, Sept. 2020.
- [6] J. Chen, L. Yang, and M.-S. Alouini, "Physical Layer Security for Cooperative NOMA Systems," *IEEE Trans. Veh. Technol.*, vol. 67, no. 5, pp. 4645–4649, May 2018.
- [7] M. Elhattab *et al.*, "Reconfigurable Intelligent Surface Enabled Full-Duplex/Half-Duplex Cooperative Non-Orthogonal Multiple Access," *IEEE Trans. Wireless Commun.*, pp. 1–1, Oct. 2021.
- [8] X. Xie *et al.*, "Ergodic Capacity and Outage Performance Analysis of Uplink Full-Duplex Cooperative NOMA System," *IEEE Access*, vol. 8, pp. 164 786–164 794, Sept. 2020.
- [9] H. Liu *et al.*, "Coordinated Uplink Transmission for Cooperative NOMA Systems," in *2018 IEEE Global Communications Conference (GLOBE-COM)*, Feb. 2019, pp. 1–6.
- [10] Y. Zhang *et al.*, "Performance analysis of a novel uplink cooperative NOMA system with full-duplex relaying," *IET Commun.*, vol. 12, no. 19, p. 2408–2417, Nov. 2018.
- [11] X. Yue *et al.*, "Exploiting Full/Half-Duplex User Relaying in NOMA Systems," *IEEE Trans. Wireless Commun.*, vol. 66, no. 2, Feb. 2018.
- [12] X. Zhang and F. Wang, "Resource Allocation for Wireless Power Transmission Over Full-Duplex OFDMA/NOMA Mobile Wireless Networks," *IEEE J. Sel. Areas Commun.*, vol. 37, no. 2, pp. 327–344, Feb. 2019.
- [13] Y. Xu *et al.*, "Joint Beamforming and Power-Splitting Control in Downlink Cooperative SWIPT NOMA Systems," *IEEE Transactions on Signal Processing*, vol. 65, no. 18, pp. 4874–4886, Sept. 2017.
- [14] E. El Haber *et al.*, "Joint Optimization of Computational Cost and Devices Energy for Task Offloading in Multi-Tier Edge-Clouds," *IEEE Trans. Commun.*, vol. 67, no. 5, pp. 3407–3421, May 2019.
- [15] Z. Wei *et al.*, "Fairness Comparison of Uplink NOMA and OMA," in *2017 IEEE 85th VTC Spring*, 2017, pp. 1–6.